Supplementary Information for "Electrical De-poling and Re-poling of Relaxor-PbTiO3 Piezoelectric Single Crystals without Heat Treatment"

Hwang-Pill Kim[1], Mao-Hua Zhang[2], Bo Wang[3], Huaiyu Wu[1], Zhengze Xu[1], Sipan Liu[1] Sunho Moon[1], Yohachi Yamashita[1,4], Jong Eun Ryu[1], Jun Liu[1], Shujun Zhang[5], Long-Qing Chen[2] and Xiaoning Jiang[1*]

[1]*Department of Mechanical and Aerospace Engineering, North Carolina State University, Raleigh, NC 27695, USA*

[2]*Department of Materials Science and Engineering, Pennsylvania State University, State College, PA 16802, USA*

[3]*Materials Science Division, Lawrence Livermore National Laboratory, Livermore, CA 94550, USA*

[4]*Department of Human and Environmental Science, Shonan Institute of Technology, Fujisawa, Kanagawa 251-8511, Japan*

[5]*Australian Institute for Innovative Materials, Institute for Superconducting and Electronic Materials, North Wollongong, New South Wales, 2500, Australia*

[*] Author to whom correspondence should be addressed: xjiang5@ncsu.edu

De-poling by direct current (DC) electric fields

In case that the direction of DC electric fields is the same with the original polarity of the ACP crystals, no de-poling was observed (**Figure S1**) since the domain alignment was reinforced.

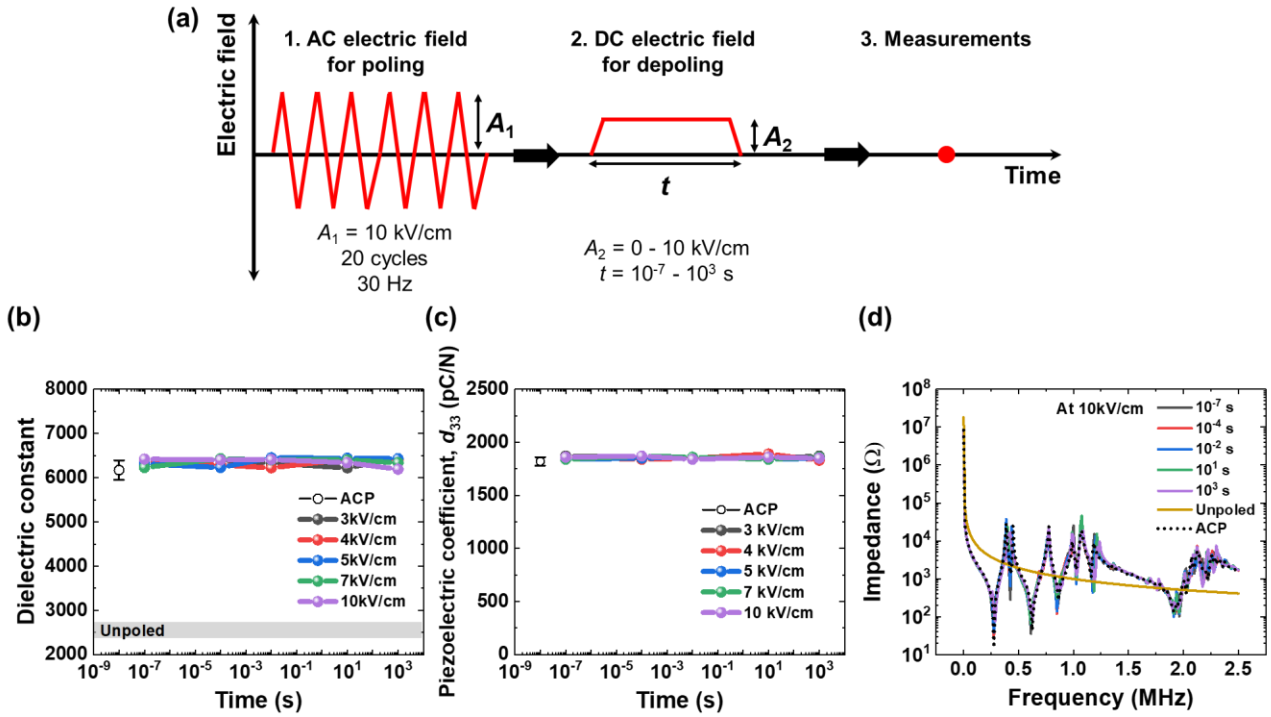

Figure S1. DC electric field de-poling for AC poled PIN-PMN-PT single crystals. (a) Schematic illustrations of experimental procedures for PIN-PMN-PT single crystals that were first poled by AC electric fields and then depoled by DC electric fields. Here, the DC electric fields for de-poling were applied along the same direction of the initial polarity of ACP crystals. (b) Dielectric constants, (c) piezoelectric coefficients, and (d) impedance spectra of the PIN-PMN-PT single crystals after applying DC electric fields for de-poling. Error bars indicate the sample standard deviation of n = 3 measurements carried out on independent samples. The amplitude and duration time of the DC electric fields were controlled to investigate their effects on the poled state in response to external electric fields.

To investigate de-poling triggered by external DC electric fields, originally AC- (ACP) and DC-poled (DCP) crystals with saturated properties were also exposed to DC electric fields that are opposite to the original polarity (**Figures S2** and **S3**). We first optimized the properties of ACP and DCP crystals, and their optimum properties (ACP: Dielectric constant = 6170 ± 220 and Piezoelectric coefficient = 1820 ± 40 & DCP: Dielectric constant = 4630 ± 100 and Piezoelectric coefficient = 1400 ± 50) are denoted in the figures for better comparisons. When DC electric fields (ranged from 3 kV/cm to 10 kV/cm mimicking the application conditions) for de-poling were in the same direction of initial polarity of ACP and DCP crystals, their properties were not changed regardless of the amplitude and duration time of DC electric fields (**Figure S1**). In the case with DC electric fields applied opposite to the original poling direction, crystal properties varied with the DC electric field amplitudes and time duration. **Figure S2b** and **S2c** show the dielectric constants and piezoelectric coefficients of ACP crystals, respectively, after DC electric fields opposite to the initial polarity were applied. The poled crystals were

partially de-poled at certain duration of times, which can be determined by decreases in their properties and variations in the impedance measurements. Shortly after the depoled state, the crystals were repoled with aligned domains along the direction of the applied DC electric fields. It should be noted that de-poling at lower amplitudes was initiated when electric fields were applied for longer time. Therefore, more duration time ($\geq$ 10 s) was required for the amplitude of 3 kV/cm, whereas considerably short time ($\leq 10^{-2}$ s) was enough to achieve a depoled state at higher electric fields which exceed their E_c (4.8 kV/cm, **Figure S2**). However, when much higher electric fields ($\geq$ 10 kV/cm) were applied for depolarization, it was hard to find a certain depolarized state because repoled states were already induced in a short period of time ($< 10^{-4}$ s). Though the relative dielectric permittivity was reduced as unpoled crystals (Dielectric constant = 2550 ± 170), several resonant modes remained (**Figure S2d**). It means a completely depoled state which occurs over a short period of time cannot be easily generated using DC electric fields. And hence, we only observed the transient depoled state at specific conditions when we applied DC electric fields for de-poling. **Figures S3b** and **S3c** present $\varepsilon^{T}_{33}/\varepsilon_0$ and d_{33} of DCP crystals, respectively, after DC electric fields opposite to initial polarity were applied. As the E_c (6.8 kV/cm) of DCP crystals are larger than the ACP crystals (**Figure S3b**), de-poling tended to be initiated by higher amplitudes of external electric fields at the same duration of time. The similar trends in the changes of the properties and impedance spectra were observed in the case of the DCP crystals. However, the conditions for a transient depoled state are different, implying that degrees of the depolarization are highly dependent on initial poling conditions (e.g. ACP or DCP).

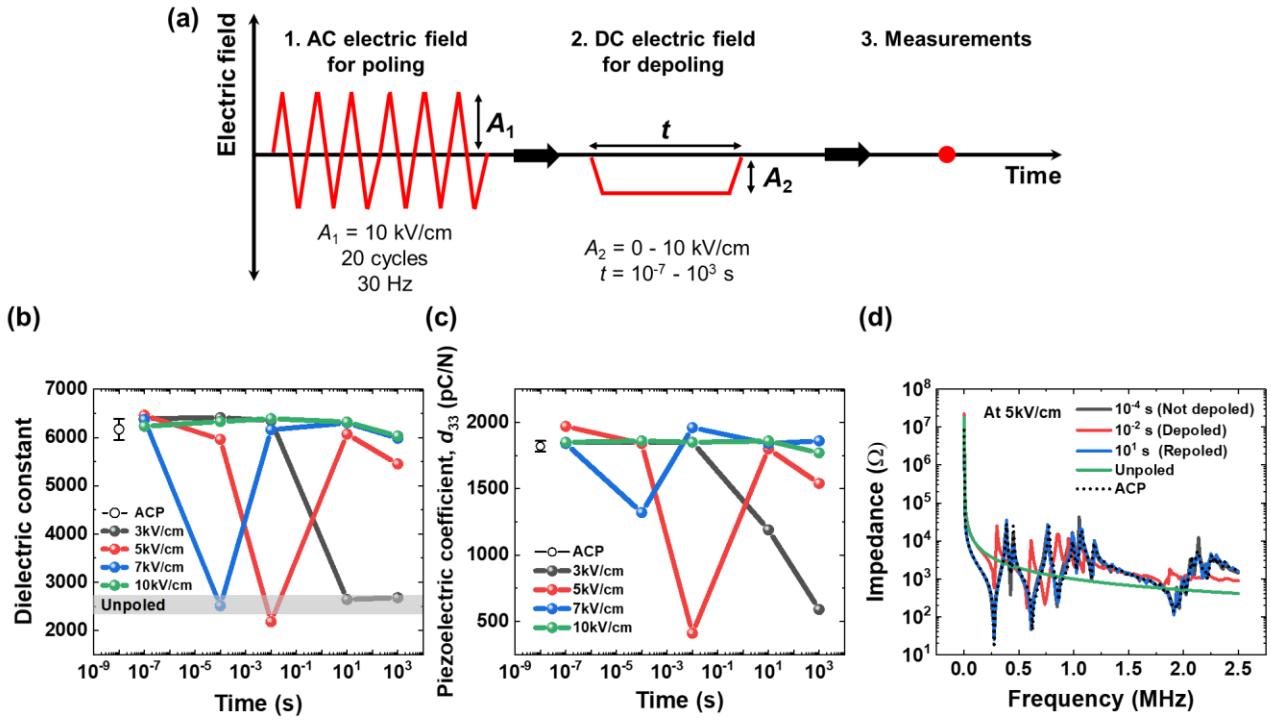

Figure S2. Opposite-direction DC electric field de-poling for AC poled PIN-PMN-PT single crystals. (a) Schematic illustrations of experimental procedures for PIN-PMN-PT single crystals that were first poled by AC electric fields and then depoled by DC electric fields. Here, the DC electric fields for de-poling were applied along the opposite direction of the initial polarity of ACP crystals. (b) Dielectric constants, (c) piezoelectric coefficients, and (d) impedance spectra of the PIN-PMN-PT single crystals after applying DC electric fields for de-poling. Error bars indicate the sample standard deviation of n = 3 measurements carried out on independent samples. The amplitude and duration time of the DC electric fields were controlled to investigate their effects

on the poled state in response to external electric fields. Though a transient depoled state can be achieved at certain amplitude and time of the electric field exposure, it is hard to find exact conditions for an almost completely depoled state using DC electric fields because de-poling occurs over a very short period of time

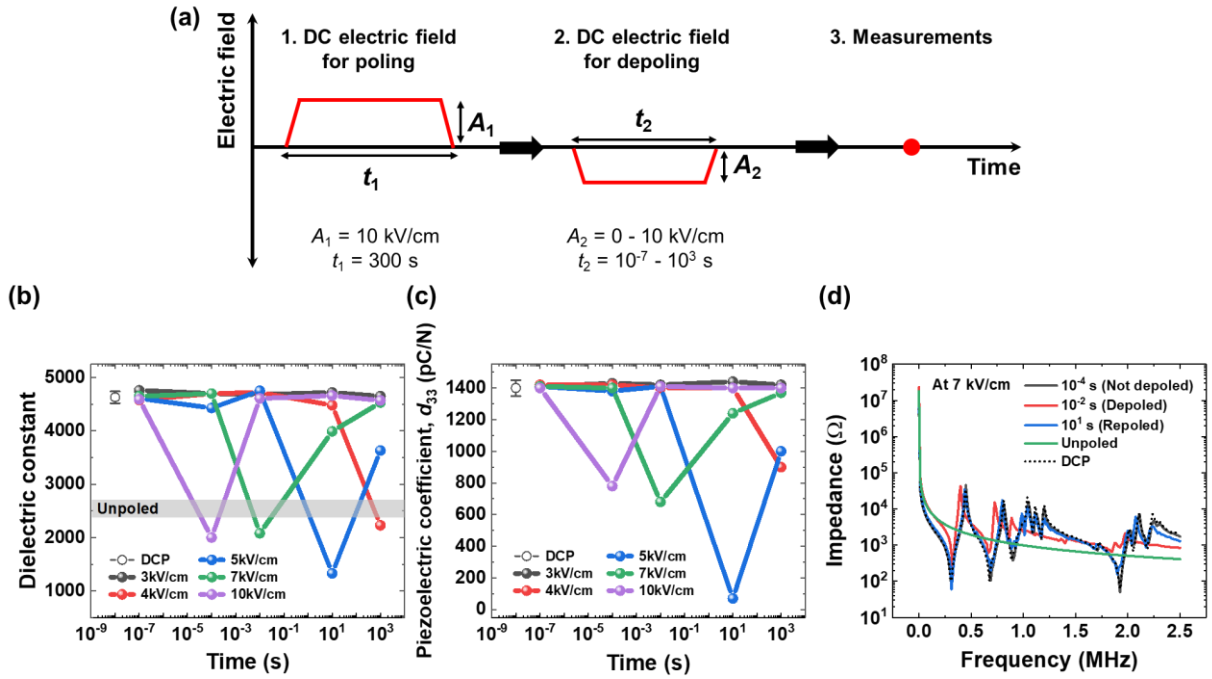

Figure S3. Opposite-direction DC electric field de-poling for DC poled PIN-PMN-PT single crystals. (a) Schematic illustrations of experimental procedures for PIN-PMN-PT single crystals that were first poled by DC electric fields and then depoled by DC electric fields. Here, the DC electric fields for de-poling were applied along the opposite direction of the initial polarity of DCP crystals. (b) Dielectric constants, (c) piezoelectric coefficients, and (d) impedance spectra of the PIN-PMN-PT single crystals after applying DC electric fields for de-poling. Error bars indicate the sample standard deviation of n = 3 measurements carried out on independent samples. The amplitude and duration time of the DC electric fields for de-poling were controlled to investigate their effects on the poled state in response to external electric fields. Here, we found that conditions for a depoled state are highly dependent on initial poled states; the amplitude and time for the DC (poling) – DC (de-poling) case are different from the AC (poling) – DC (de-poling) case shown in **Figure S2**.

Polarization hysteresis loops and electric fields induced current measurements

Polarization hysteresis loops and electric field induced current measurements were conducted to study the poled and depoled states (**Figures S4**, **S5**).

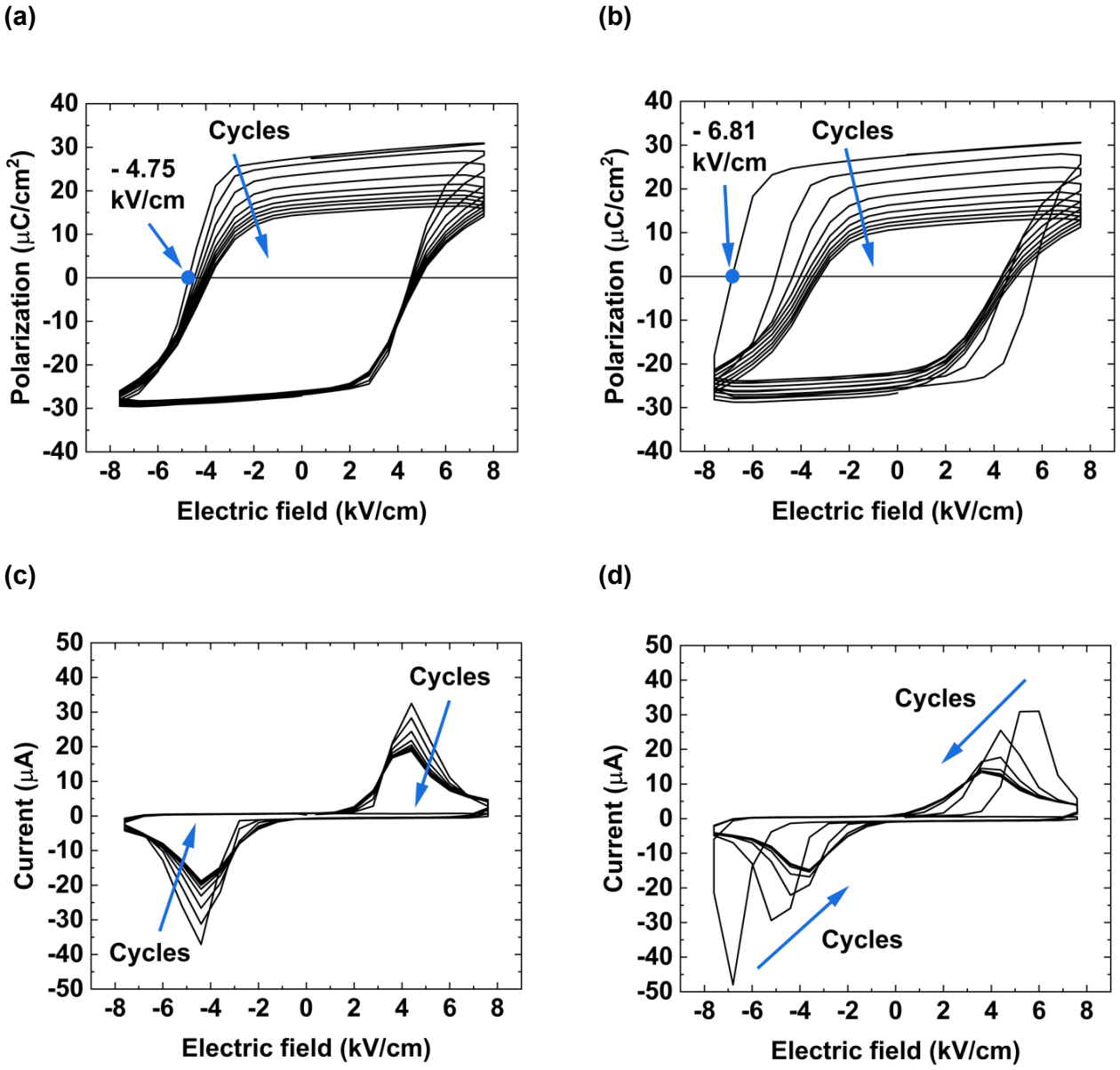

Figure S4. Polarization hysteresis loops and electric fields induced current measurements of electric de-poling (peak amplitude of 8 kV/cm, 10 cycles and 1 Hz). Polarization hysteresis loops of (a) ACP and (b) DCP PIN-PMN-PT crystals during 10 successive bi-polar cycles at 1 Hz. Electric field induced current curves of (c) ACP and (d) DCP PIN-PMN-PT crystals during 10 successive bi-polar cycles at 1 Hz.

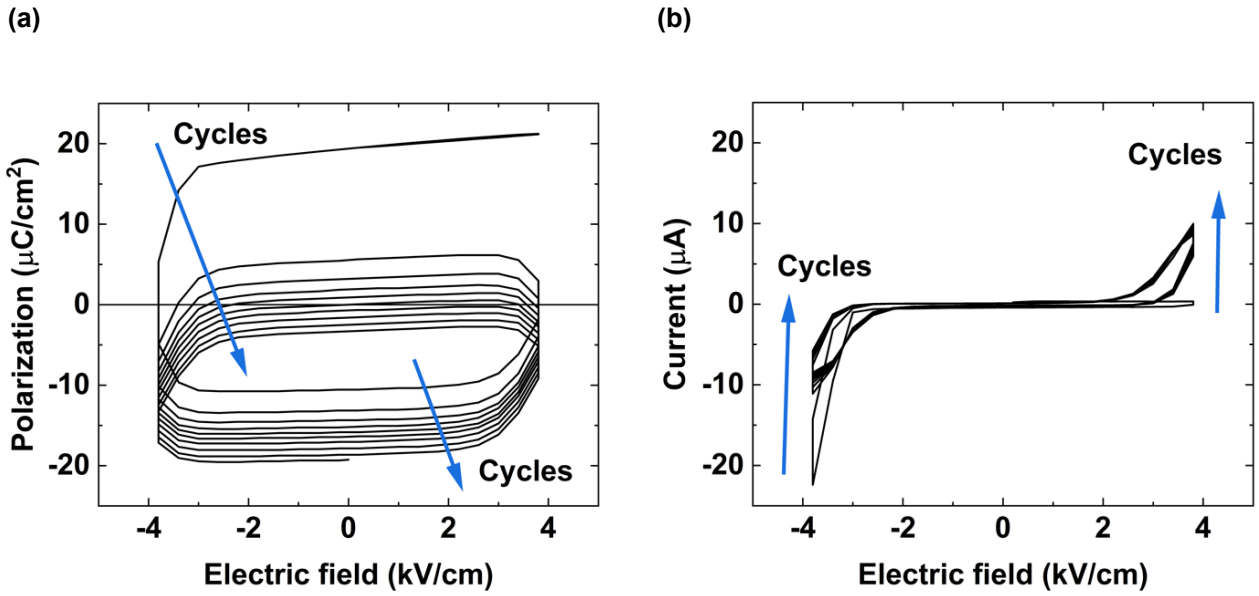

Figure S5. Polarization hysteresis loops and electric fields induced current measurements of electric de-poling (peak amplitude of 4 kV/cm, 10 cycles and 1 Hz). (a) Polarization hysteresis loops and (b) electric field induced current curves of ACP PIN-PMN-PT crystals during 10 successive bi-polar cycles at 1 Hz. Here, a condition for fully depoled states was used to measure these ferroelectric properties.

Phase field simulation

Material properties used in the simulation are given in **Table S1**. The simulated domain structures of the unpoled, ACP and DCP crystals are shown in **Figure S6.** Evolution of the domain structures of an ACP crystal sample exposed to an AC electric field with amplitude of ~ 0.85E_c can be found in the video file.

Supplementary Table 1. Material coefficients of PMN-30PT employed for phase-field simulations.

Coefficient	Value	Coefficient	Value
a_1	$(2.295T - 935.9) \times 10^5$ J mC^{-2}	c_{11}	1.92×10^{10} J m^{-3}
a_{11}	$(-0.3775T + 457.7) \times 105$ J m^{5}C^{-4}	c_{12}	5.29×10^{10} J m^{-3}
a_{12}	6.075×10^7 J m^{5}C^{-4}	c_{44}	7.14×10^{10} J m^{-3}
a_{111}	2.57×10^7 J m^{9}C^{-6}	Q_{11}	0.084 m^{4}C^{-2}
a_{112}	6.95×10^9 J m^{9}C^{-6}	Q_{12}	−0.025 m^{4}C^{-2}
a_{123}	13.13×10^9 J m^{9}C^{-6}	Q_{44}	0.035 m^{4}C^{-2}
P	0.50 Cm^{-2}	g_{11}	0.1×10^{-10} J m^{3}C^{-2}
T_C	408 K	g_{12}	-0.1×10^{-10} J m^{3}C^{-2}
κ	50	g_{44}	0.1×10^{-10} J m^{3}C^{-2}

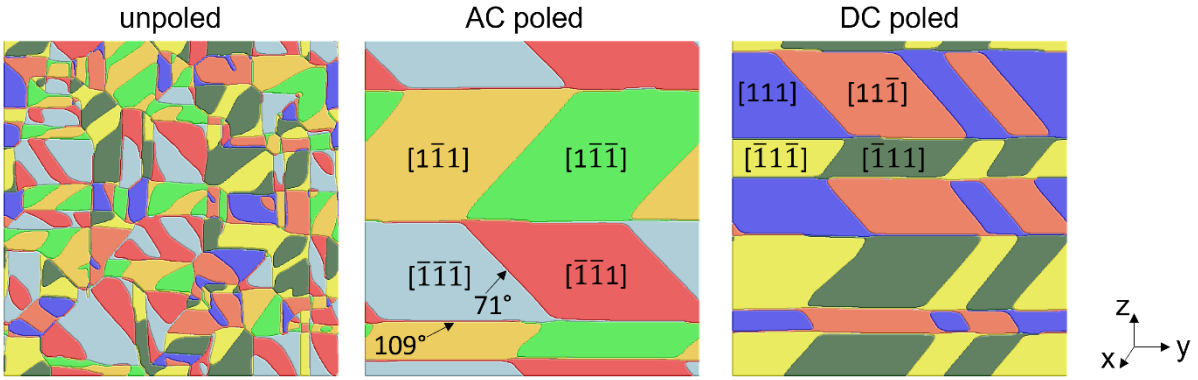

Figure S6. Simulated domain structures of the studied materials in the (a) unpoled state, (b) ACP, and (c) DCP. The 180° domains in the unpoled state are eliminated in the ACP and DCP samples, resulting in a mixture of 71° and 109° domain walls. The domains with identical polarization vectors have the same colors. The horizontal layers of the poled samples are separated by a set of 109° domain walls parallel to the (001) plane, and within each layer the 71° domain walls are approximately parallel to (011) planes. The ACP sample has a significantly lower domain wall density than the DCP sample.

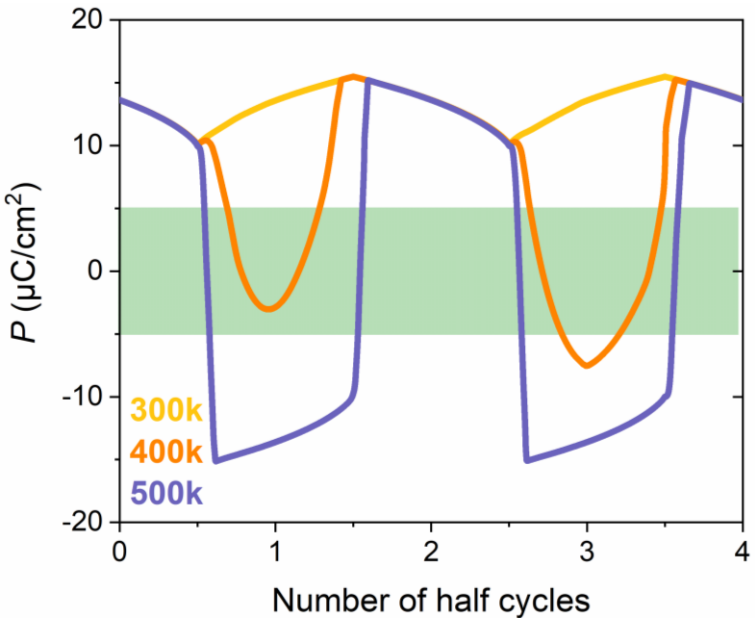

Figure S7. Polarization as a function of the number of cycles of the investigated sample exposed to AC electric fields of 53.3 kV/cm (0.85 E_C) at different AC periods, *i.e.*, 300 k timesteps, 400 k timesteps, and 500 k timesteps per cycle, corresponding to high, medium, and low frequencies, respectively. The simulation agrees qualitatively well with the experimental observation. As seen in the blue line of **Figure 1c**, the sample remains poled when exposed to 4 kV/cm at a frequency higher than 10^3 Hz, while the sample is not well de-poled when exposed to 4 kV/cm at a frequency of 10^{-2} Hz.

Visualization of ferroelectric domains

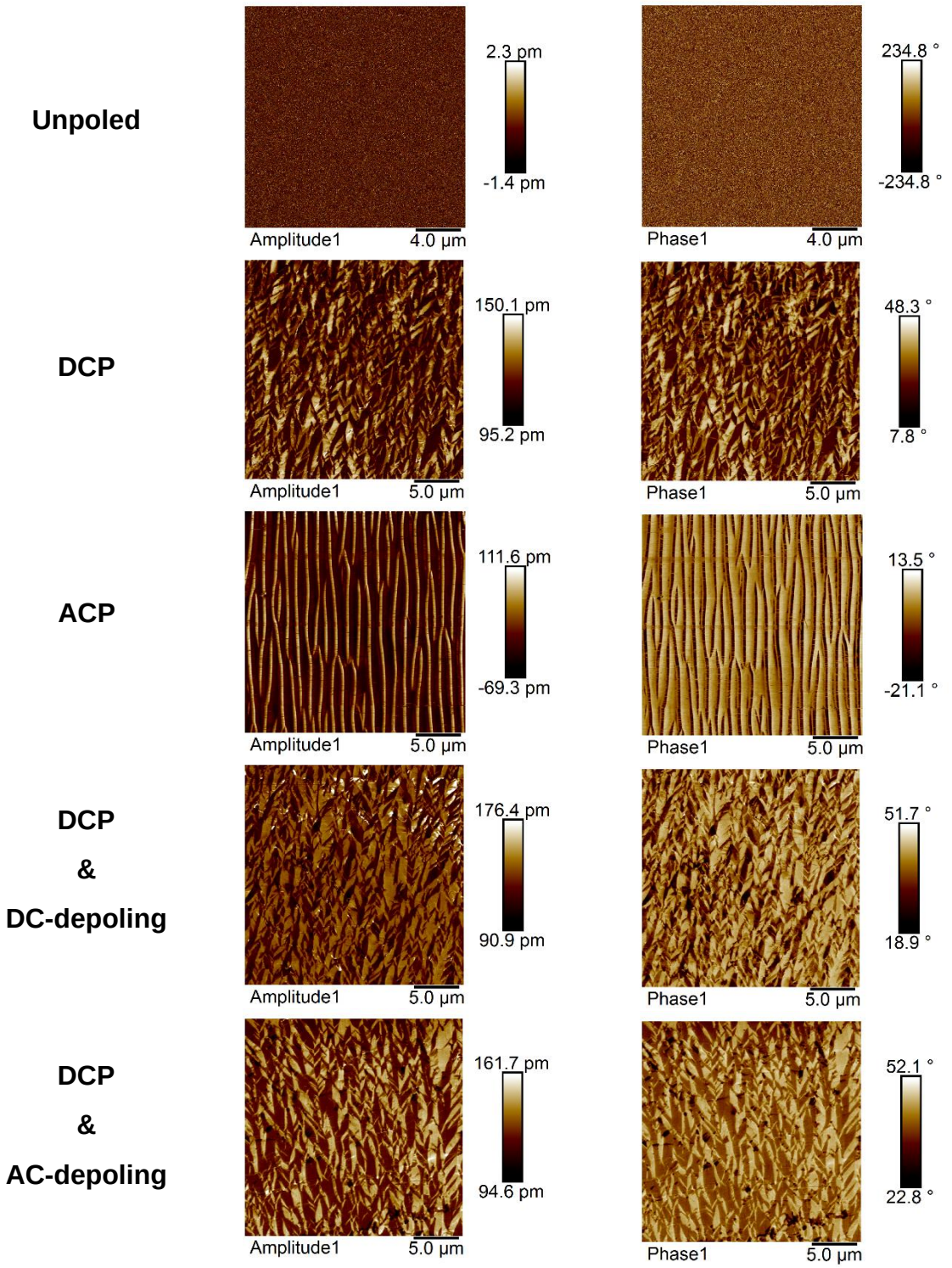

Figure S8. Piezoresponse force microscopy (PFM) amplitude and phase images of unpoled, DCP, ACP, DC-depoled and AC-depoled PIN-PMN-PT crystals. Given that our simulation results show that electrically-depoled crystals have irregular patterns similar to DC-poled crystals to some extent, our PFM results are well consistent with the computational calculations.

X-ray diffraction patterns (XRD)

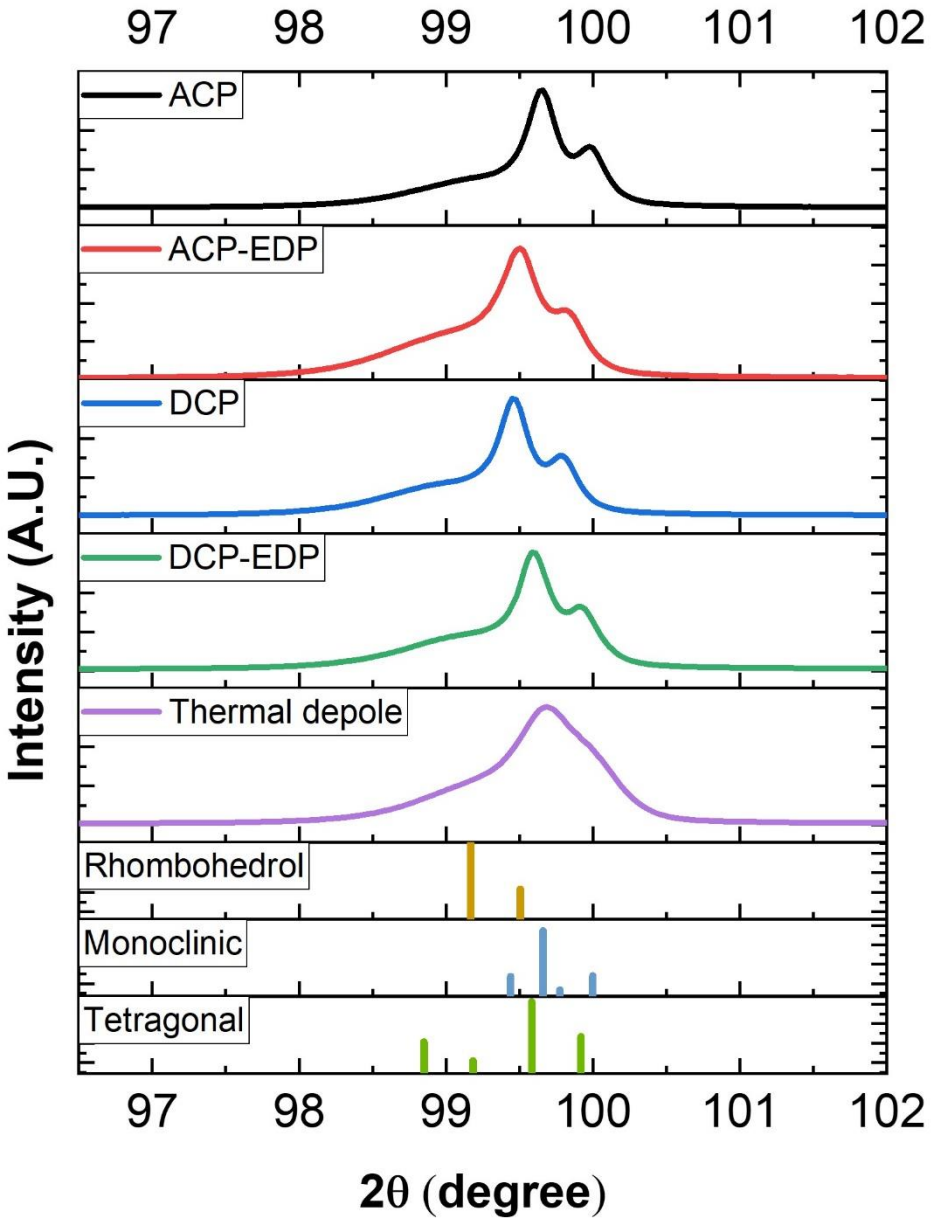

Figure S9. X-ray diffraction (400) patterns of the PIN-PMN-PT single crystals at different poling conditions including ACP, ACP-EDP, DCP, DCP-EDP and thermal depoled state. The intensities have been normalized and reference patterns are shown in the bottom.

Demonstration of reversible re-poling and de-poling of PIN-PMN-PT single crystals in device

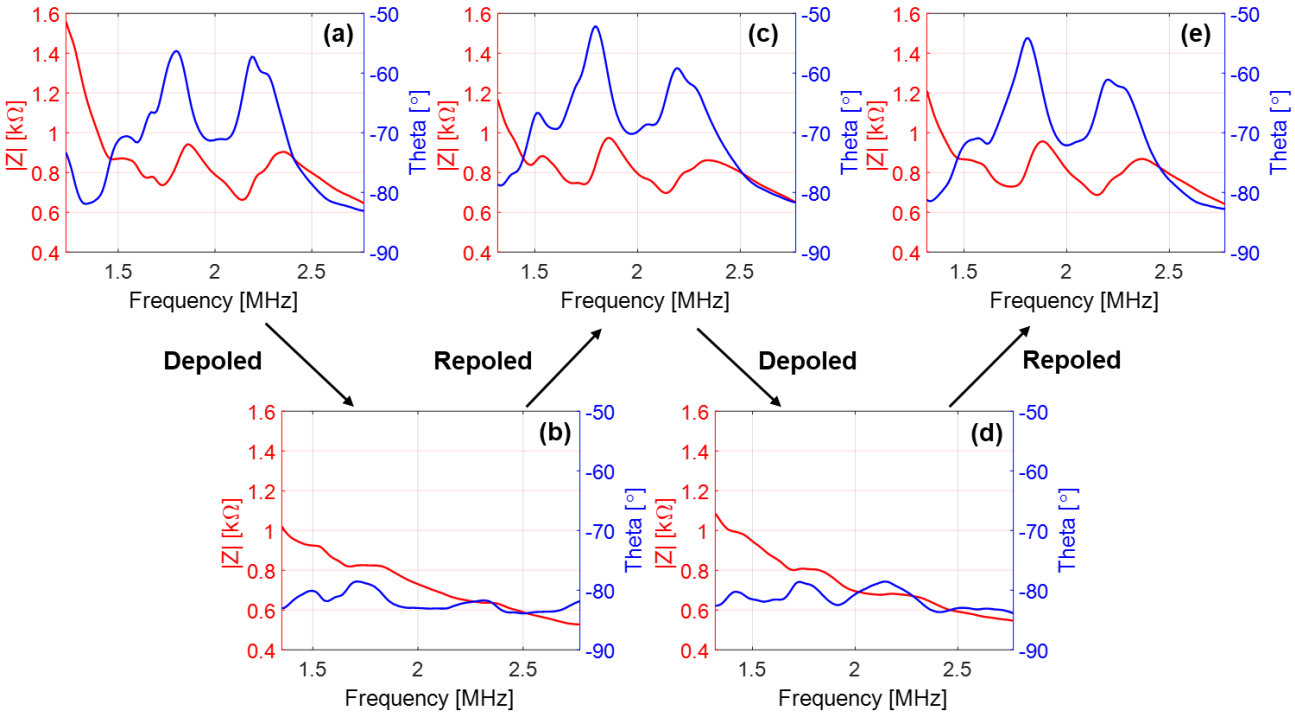

Figure S10. Impedance/phase spectra of the transducer at the different stages of the in-device de-poling and re-poling processes under AC electric fields: (a) Original status (ACP), (b) First depoled state, (c) First repoled state, (d) Second depoled state, and (e) Second repoled state. The device showed the consistent electrical impedance of 800 Ω @ 2 MHz ((a),(c),(e)). The capacitance varied from 484 pF to 457 pF after the second re-poling, which indicates a negligible deviation of 5%. The device also showed negligible resonances at depoled states ((b)&(d))

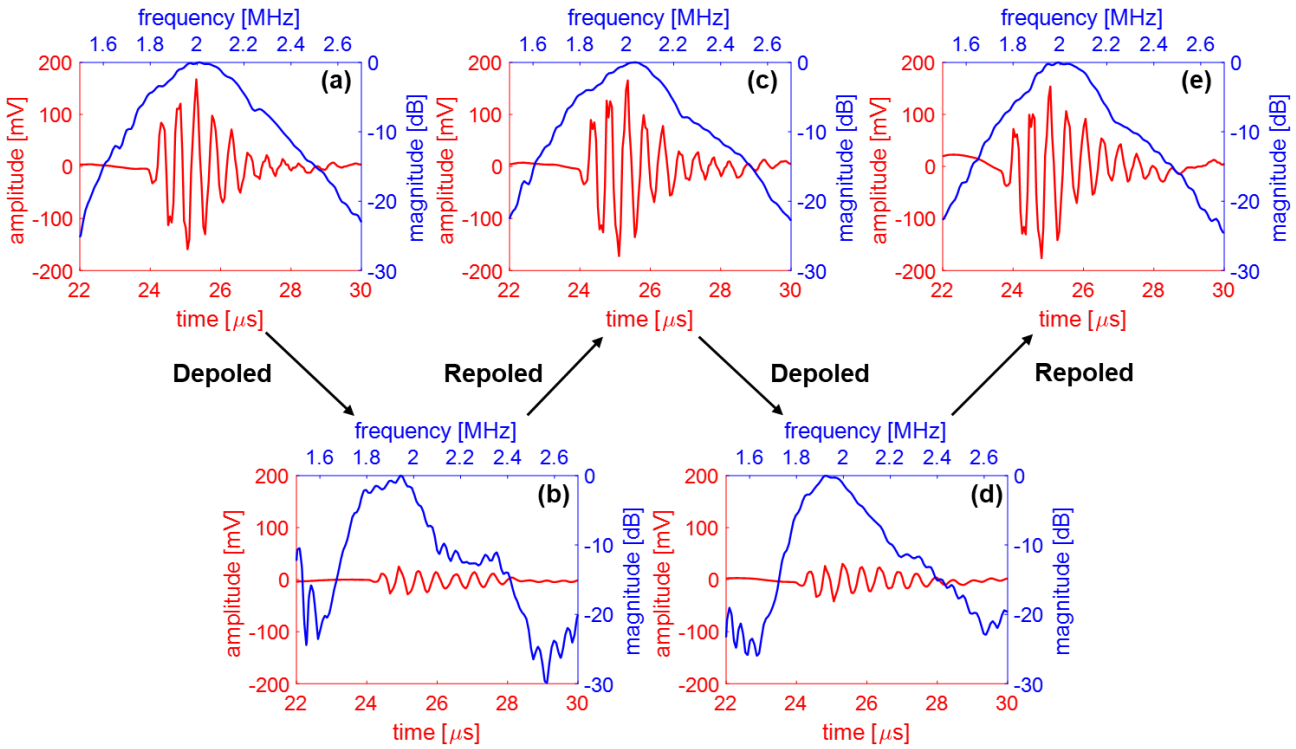

Figure S11. Pulse/echo response at different stages of the in-device de-poling and re-poling processes under AC electric fields: (a) Original status (ACP), (b) First depoled state, (c) First repoled state, (d) Second depoled state, and (e) Second repoled state. The device showed a consistent waveform after each re-poling process (a)(c)(e). Compared with the depoled states ((b)(d), averaged 40 mV_{pp}), the repoled sample showed a significant sensitivity difference ((c) and (e), averaged 361 mVpp). It is noted that after the second re-poling, the peak-to-peak value increased from 327 mV to 397 mV, which may be due to the transducer/hydrophone alignment error during the test.

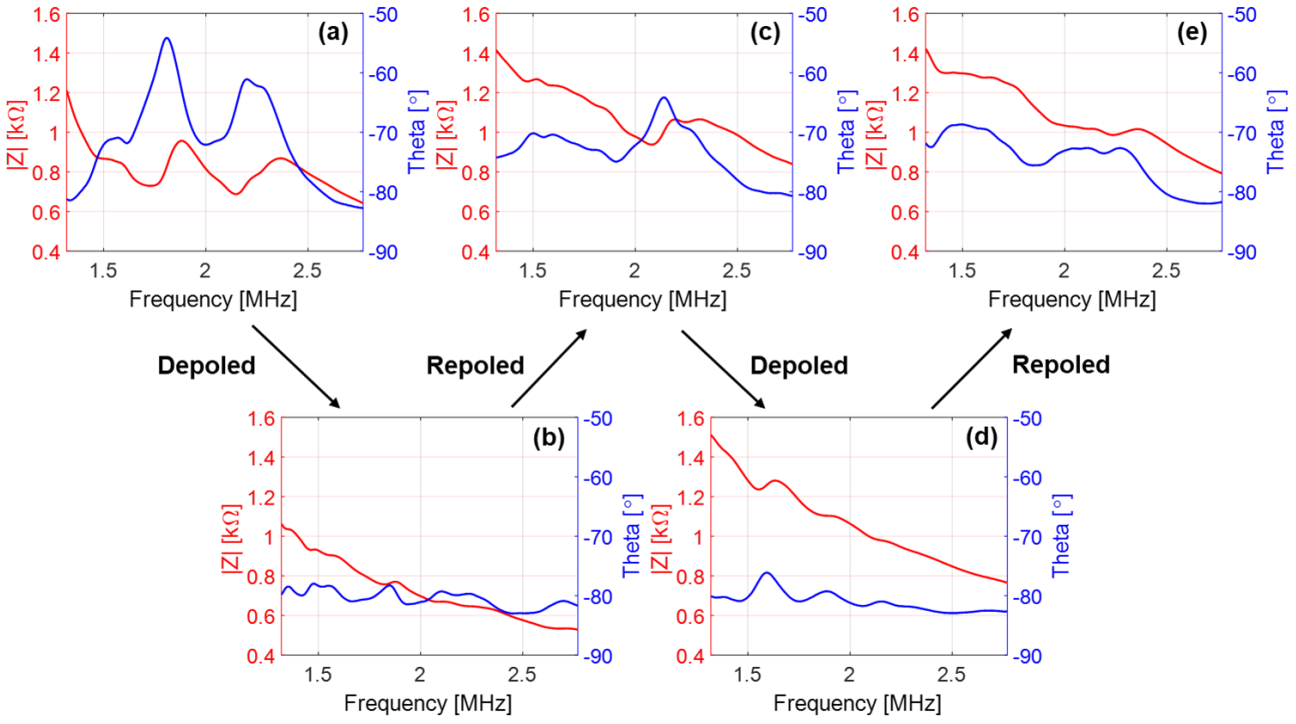

Figure S12. Impedance/phase spectra of the transducer at different stages of in-device de-poling and re-poling processes under DC electric fields: (a) Original status (DCP), (b) First de-poling, (c) First re-poling, (d) Second

de-poling, and (e) Second re-poling. The repoled sample (c)(e) showed a significant difference compared with the original results (a). The capacitance dropped dramatically by 49.6% and the dielectric loss increased from 0.2% to 1.9%, indicating the partial failure of the device after DC electric fields induced de-poling/re-poling processes.

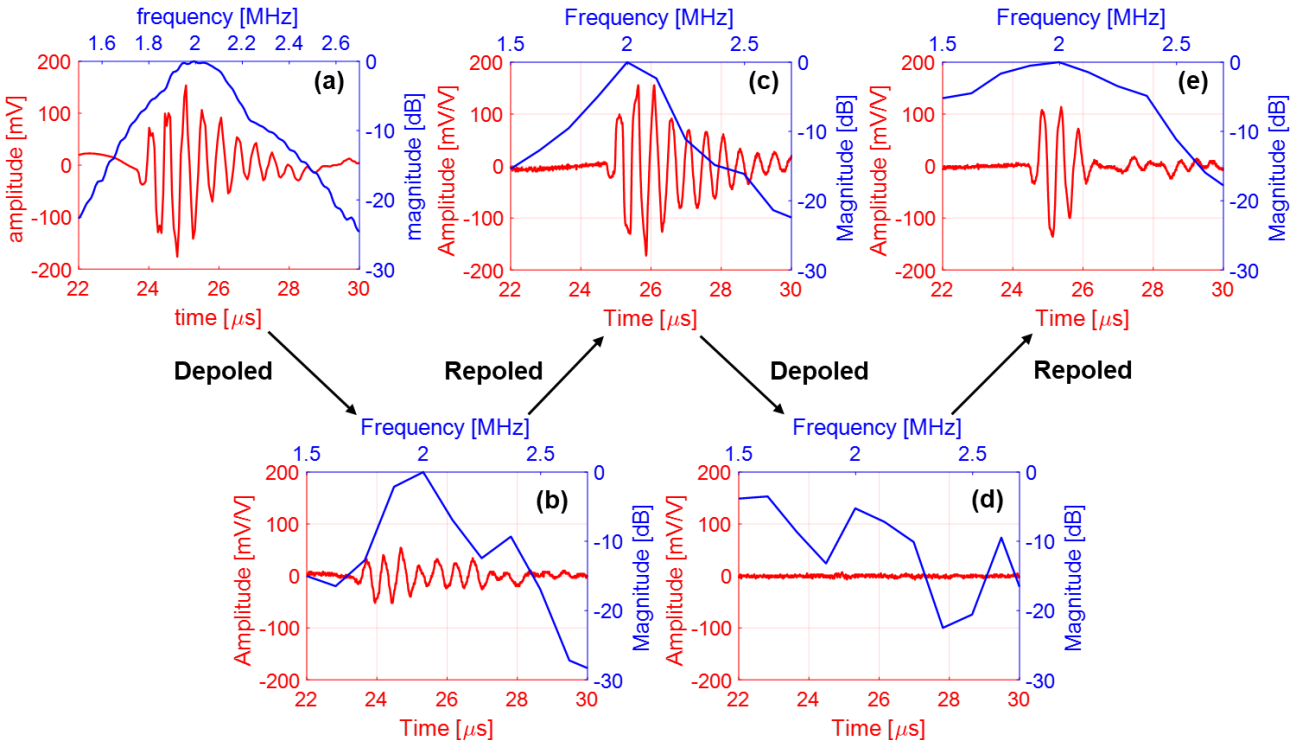

Figure S13. Pulse/echo responses of the transducers at different stages of in-device de-poling and re-poling processes under DC electric fields: (a) Original status (DCP), (b) First de-poling, (c) First re-poling, (d) Second de-poling, and (e) Second re-poling. The peak-to-peak voltage dropped from 396 mV (a) to 250 mV (e), or by 36.8%, after the second re-poling.

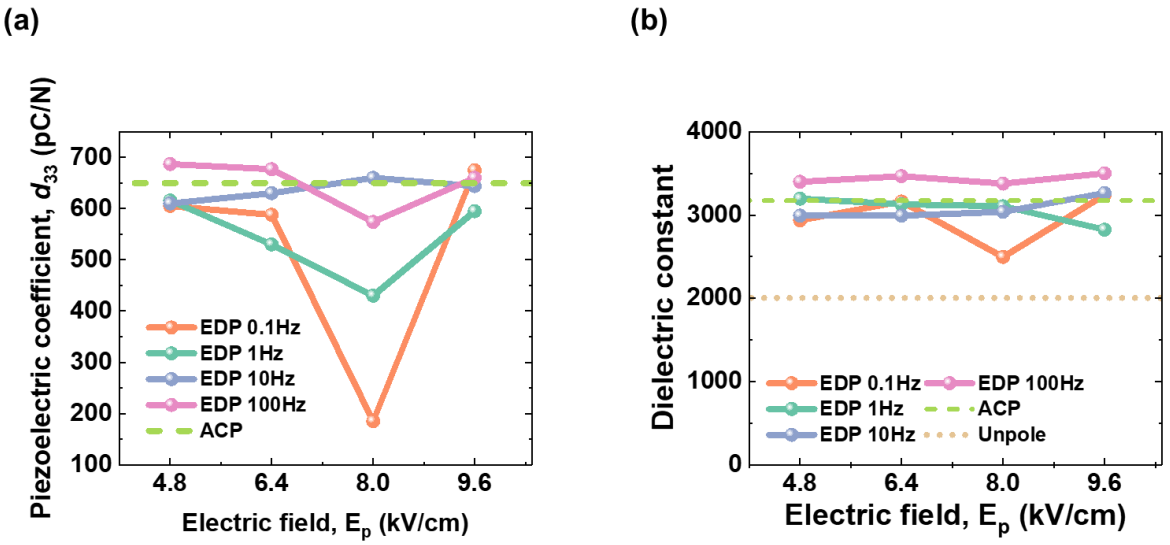

Figure S14. AC electric de-poling tests for $Pb(Zr,Ti)O_3$ ceramics. (a) Piezoelectric coefficients and (b) dielectric constants of poled $Pb(Zr,Ti)O_3$ ceramics after applying AC electric fields for de-poling. The peak

amplitudes and frequencies of the AC electric fields for de-poling were varied to investigate how poled states change in response to external electric fields. The dimension of the samples is $3 \times 3 \times 0.9t$ mm^3, which is similar to that of the crystals in this work. Given that its E_c is close to 8 kV/cm, an electric poling condition is set as 12.5 kV_{pp}/cm, 1 Hz and 20 cycles while electric fields for de-poling were applied under different frequencies (0.1, 1, 10 and 100 Hz) and amplitudes (0.6, 0.8, 1.0 and 1.2 E_c) at a fixed cycle (10 cycles).

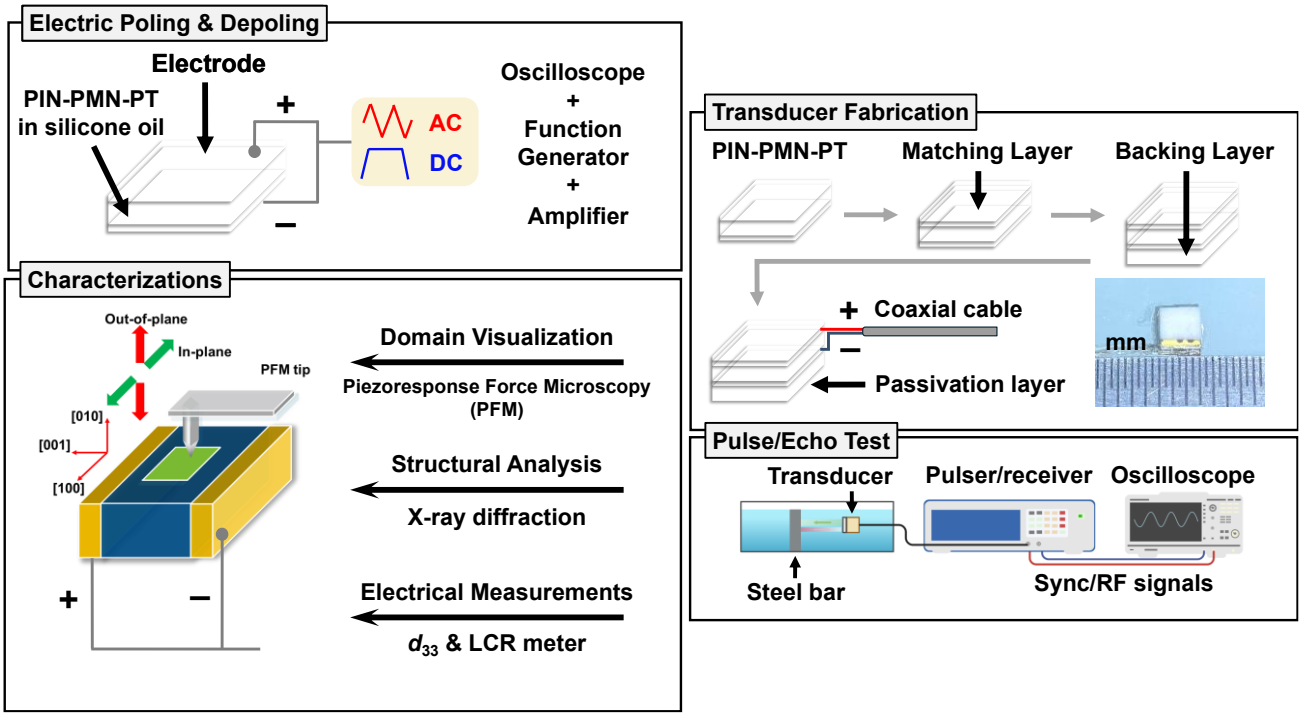

Figure S15. Schematic illustrations depicting the experimental procedures and characterizations in this work.